INFINITE-HORIZON PREDICTIVE CONTROL OF A HELICOPTER MODEL WITH THREE DEGREES OF FREEDOM

Rubens Junqueira Magalhães Afonso, rubensjma@gmail.com
Roberto Kawakami Harrop Galvão, kawakami@ita.br
Instituto Tecnológico de Aeronáutica, Divisão de Engenharia Eletrônica, 12228-900, São José dos Campos - SP

Abstract. *This paper investigates the potential benefits of using an infinite-horizon formulation of Model-based Predictive Control (MPC) for a three-degrees of freedom (3DOF) helicopter model. The infinite-horizon formulation guarantees nominal closed-loop stability of the system. Moreover, if the prediction model is linear and the constraints over the states and inputs are given as linear inequalities, then the cost function can be written in a form that involves a finite horizon and a terminal cost. Under these hypotheses, it can also be shown that state constraints only need to be imposed over a finite number of steps in order to guarantee constraint satisfaction over the infinite horizon. The resulting optimization problem involves a finite number of decision variables and constraints. Therefore, Quadratic Programming techniques can be employed to obtain the optimal control at each sampling time. The present study is carried out by using a nonlinear simulation model of a 3DOF helicopter. The investigation is mainly concerned with robustness of the controller regarding possible failures in the helicopter motors. Such failures are modeled as gain changes in the actuators. The results are evaluated through simulations in the Matlab/Simulink environment. For this purpose, the transient response of the closed-loop system and the satisfaction of state constraints are considered. For comparison, a finite-horizon MPC formulation is also employed.*

Keywords: *predictive control; infinite-horizon; stability*

1. INTRODUCTION

1.1 Model-based Predictive Control

Model-based Predictive Control (MPC) techniques consist of solving a moving-horizon optimal control problem. Such a solution is reiterated at periodic intervals (normally at each sample period) based on sensor feedback information (Camacho and Bordons, 1999), (Rossiter, 2003). Historically, this strategy was developed to cope with the demands of the petrol industry (Cutler and Ramaker, 1980), but its application to other fields is currently increasing (Qin and Badgwell, 2003). One of the main advantages of Predictive Control is the ability to deal with constraints over the inputs and states of the plant (Maciejowski, 2002).

Figure 1 depicts the basic elements of a predictive controller, which are:

- A model employed to predict the state of the plant over a horizon of N steps in the future, based on the current state $x(k)$ and the control sequence to be applied.
- An algorithm for optimization of the control sequence $\{\hat{u}(k+i|k), i = 0, 1, \ldots, N-1\}$, considering a designated cost function for the problem and the constraints over the inputs and states of the plant.

In regulation problems, the cost function is typically of the form

$$J[\hat{u}(k|k), \hat{u}(k+1|k), \ldots, \hat{u}(k+N-1|k)] = \sum_{i=1}^{N} \|\hat{x}(k+i|k)\|_Q^2 + \|\hat{u}(k+i-1|k)\|_R^2 \quad (1)$$

in which $\|x\|_Q^2 = x^T Q x$ and $\|u\|_R^2 = u^T R u$, with $Q \geq 0$ and $R > 0$ being the weight matrices adjusted by the designer.

Such a cost may be defined over an infinite-horizon as in (Maciejowski, 2002) in order to guarantee closed-loop stability.

In this work the cost function of Eq. (1) with infinite-horizon was adopted and its advantages when compared to a standard finite horizon formulation were studied.

Regarding constraint enforcement, if the prediction model is linear and the constraints over states and control are given as linear inequalities, it can be proven (Rawlings and Muske, 1993) that there exists a finite horizon (N_1) over which the constraints must be enforced to ensure that they will be enforced at all future times.

The present paper investigates the potential benefits of using an infinite-horizon formulation of Model-based Predictive Control (MPC) for a three-degrees of freedom (3DOF) helicopter model. Simulation results of the control of the nonlinear helicopter model pre-stabilized by state feedback were compared for the finite and infinite-horizon controllers. A model mismatch was simulated by diminishing the voltage gain of one of the helicopter motors. The output of the plants were compared regarding deviation from the nominal behavior and enforcement of constraints.

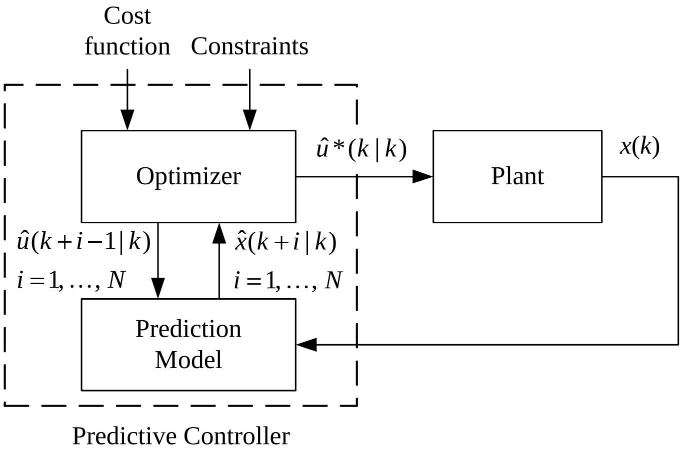

Figure 1. Predictive control loop employing state feedback. In this figure, $u \in \mathbb{R}^p$ and $x \in \mathbb{R}^n$ denote the input and state variables of the plant, respectively. Moreover, $\hat{x}(k+i|k)$ represents the predicted state value at time $(k+i)$ calculated on the basis of the current state $x(k)$. The optimal control to be applied to the plant at time k is denoted by $\hat{u}^*(k|k)$.

The remaining sections are organized as follows. Section 2 describes the infinite-horizon MPC formulation adopted in this work as well as the formulation of the constraints over inputs and states as linear inequalities involving the optimal control produced by the MPC controller. Section 3 presents the 3DOF-helicopter nonlinear simulation model, the linearized model used as reference in the MPC controller and also the proposed algorithm used to find the finite constraint horizon (Rawlings and Muske, 1993). Next, section 4 presents the simulation results and a comparative analysis of the finite and infinite-horizon formulations. Finally, concluding remarks are given in section 5.

2. PREDICTIVE CONTROL FORMULATION

Using a shortened notation, the cost given in Eq. (1) is usually denoted by $J(k)$, clarifying that this is the function to be optimized at the k^{th} sample period. If the prediction model is linear:

$$\hat{x}(k+i|k) = \begin{cases} x(k),\ i=0 \\ A\hat{x}(k+i-1|k) + B\hat{u}(k+i-1|k),\ i>0 \end{cases} \tag{2}$$

and the constraints are represented as linear inequalities over the control and states:

$$\begin{cases} S_u\hat{u}(k+i-1|k) \leq b_u,\ i=1,\ldots,N \\ S_x\hat{x}(k+i|k) \leq b_x,\ i=1,\ldots,N \end{cases} \tag{3}$$

then Quadratic Programming algorithms (Camacho and Bordons, 1999), (Maciejowski, 2002) may be employed to obtain the optimal control sequence $\{\hat{u}^*(k+i-1|k), i=1,\ldots,N\}$. The first element of this sequence $(u(k) = \hat{u}^*(k|k))$ is applied to the plant and the optimization is repeated at the next sample period, with $u(k+1) = \hat{u}^*(k+1|k+1)$. Such a strategy is known as *receding horizon* (Rossiter, 2003).

Nominal stability of the control loop can be guaranteed through the introduction of a terminal constraint $\hat{x}(k+N|k) = 0$, provided that the resulting optimization problem is feasible (Keerthi and Gilbert, 1988), (Mayne, Rawlings, Rao *et al.* 2003). An alternative approach for ensuring stability consists of employing a cost function with infinite prediction horizon (Maciejowski, 2002):

$$J(k) = \sum_{i=0}^{\infty} \|\hat{x}(k+i|k)\|_Q^2 + \|\hat{u}(k+i|k)\|_R^2 \tag{4}$$

subject to

$$S_u\hat{u}(k+i|k) \leq b_u,\ i=0,1,\ldots,N-1 \tag{5}$$

$$S_x\hat{x}(k+i|k) \leq b_x,\ i \geq 1 \tag{6}$$

$$\hat{u}(k+i|k) = 0,\ i \geq N \tag{7}$$

If the prediction model is of the form presented in Eq. (2), and the control is set to zero after N steps, as imposed in Eq.(7), it follows that:

$$\hat{x}(k+N+j|k) = A^j\hat{x}(k+N|k),\ j=0,1,\ldots \tag{8}$$

Using Eq. (8), the sum involving the states in Eq. (4) can be rewritten as:

$$\sum_{i=0}^{\infty} \|\hat{x}(k+i|k)\|_Q^2 = \sum_{i=0}^{N-1} \|\hat{x}(k+i|k)\|_Q^2 + \sum_{i=N}^{\infty} \|\hat{x}(k+i|k)\|_Q^2 \tag{9}$$

The second term in the right-hand side of Eq. (9) is then calculated with aid of Eq. (8) as:

$$\begin{aligned} &\textstyle\sum_{i=N}^{\infty} \|\hat{x}(k+i|k)\|_Q^2 = \sum_{j=0}^{\infty} \hat{x}^T(k+N|k)(A^j)^T Q (A^j)\hat{x}(k+N|k) = \\ &= \hat{x}^T(k+N|k)\Big[\textstyle\sum_{j=0}^{\infty}(A^j)^T Q (A^j)\Big]\hat{x}(k+N|k) \end{aligned} \tag{10}$$

Therefore, the cost in Eq. (4) can be rewritten as:F

$$J(k) = \hat{x}^T(k+N|k)\bar{Q}\hat{x}(k+N|k) + \sum_{i=0}^{N-1} \|\hat{x}(k+i|k)\|_Q^2 + \|\hat{u}(k+i|k)\|_R^2 \tag{11}$$

where

$$\bar{Q} = \sum_{j=0}^{\infty}(A^j)^T Q (A^j) \tag{12}$$

provided that the eigenvalues of A are inside the unit circle (Muske and Rawlings, 1993). From Eq. (12):

$$A^T\bar{Q}A = \sum_{j=1}^{\infty}(A^j)^T Q (A^j) = \bar{Q} - Q \tag{13}$$

Therefore, $\bar{Q}$ is the solution of the following Lyapunov equation:

$$A^T\bar{Q}A - \bar{Q} + Q = 0 \tag{14}$$

Thus, the cost function form Eq. (11) involves a finite horizon of N steps and a terminal cost term. Moreover, it can be shown (Rawlings and Muske, 1993) that $\exists N_1 > 0$ such that $S_x\hat{x}(k+i|k) \le b_x,\ i = 1, \dots, N_1 \Rightarrow S_x\hat{x}(k+i|k) \le b_x,\ \forall i > N_1$. As a result, the number of constraints to be imposed becomes finite, which allows the use of Quadratic Programming algorithms for obtaining the optimal control sequence.

This infinite-horizon approach can also be employed for plants with unstable dynamics. However, it must be imposed that the unstable modes must be taken to zero until the end of the horizon of N steps. Alternatively, an internal loop can be employed to stabilize the plant, leaving for the predictive controller the task of providing the reference signal for this loop (Chisci, Rossiter and Zappa, 2001). In this case, the control law assumes the form:

$$u(k) = -Kx(k) + v(k) \tag{15}$$

with $v(k)$ being the signal generated by the predictive controller. Matrix A must then be replaced by $\tilde{A} = A - BK$ and the constraints over the signal $u(k)$ must be written in terms of constraints over $v(k)$. This is the approach adopted in the present work.

2.1 Matrix formulation

In order to use a more concise notation, the following column vectors are introduced:

$$\hat{X} = \begin{bmatrix} \hat{x}(k+1|k) \\ \vdots \\ \hat{x}(k+N|k) \end{bmatrix}_{nN\times 1}, \quad \hat{V} = \begin{bmatrix} \hat{v}(k|k) \\ \vdots \\ \hat{v}(k+N-1|k) \end{bmatrix}_{pN\times 1} \tag{16}$$

A modified version of the cost function (11) can be obtained by removing the term containing $\hat{x}(k|k) = x(k)$, which is a constant value in the optimization process. The modified cost may be written as

$$J_{mod} = \hat{X}^T\mathcal{Q}\hat{X} + \hat{V}^T\mathcal{R}\hat{V} \tag{17}$$

where:

$$\mathcal{Q} = \begin{bmatrix} Q & 0 & \cdots & 0 \\ 0 & Q & \cdots & 0 \\ \vdots & \vdots & \ddots & \vdots \\ 0 & 0 & \cdots & \bar{Q} \end{bmatrix}_{nN\times nN}, \quad \mathcal{R} = \begin{bmatrix} R & 0 & \cdots & 0 \\ 0 & R & \cdots & 0 \\ \vdots & \vdots & \ddots & \vdots \\ 0 & 0 & \cdots & R \end{bmatrix}_{pN\times pN} \tag{18}$$

Given a linear model as in Eq. (2) and a control law of the form of Eq. (15), a prediction equation for the state can be written as:

$$\hat{X} = H\hat{V} + \hat{F} \tag{19}$$

where:

$$H = \begin{bmatrix} B & 0 & \cdots & 0 \\ \tilde{A}B & B & \cdots & 0 \\ \vdots & \vdots & \ddots & \vdots \\ \tilde{A}^{N-1}B & \tilde{A}^{N-2}B & \cdots & B \end{bmatrix}, \quad \hat{F} = \begin{bmatrix} \tilde{A} \\ \tilde{A}^2 \\ \vdots \\ \tilde{A}^N \end{bmatrix} x(k) \tag{20}$$

and $\tilde{A} = A - BK$, which corresponds to the state equation matrix for the inner closed-loop system. Finally, by substituting $\hat{X}$ in (17) with the expression in (19), the cost can be rewritten as:

$$J_{mod} = \hat{V}^T(H^T \mathcal{Q} H + \mathcal{R})\hat{V} + 2\hat{F}^T \mathcal{Q} H \hat{V} + \hat{F}^T \mathcal{Q} \hat{F} \tag{21}$$

Since Eq. (21) is quadratic in terms of $\hat{V}$, Quadratic Programming algorithms (Maciejowski, 2002) can be used to obtain the optimal control sequence $\{\hat{v}^*(k+i|k), i = 0, 1, \ldots, N-1\}$. For this purpose, the state and input constraints must be expressed as linear inequalities involving $\hat{V}$, as described in the next subsections.

2.2 State Constraints

As demonstrated in (Rawlings and Muske, 1993), there exists a finite horizon $N_1 = N + k_2$ such that, if the state constraints are enforced over this horizon, they will also be enforced in all future times. Therefore, given lower and upper bounds on the state (x_{min} and x_{max}, respectively), it is sufficient to impose:

$$H_l \leq \hat{X}_{k_2+N} = \begin{bmatrix} \hat{X} \\ \hat{x}(k+N+1|k) \\ \vdots \\ \hat{x}(k+N+k_2|k) \end{bmatrix} \leq H_u \tag{22}$$

where H_l and H_u are given as $H_l = \begin{bmatrix} x_{min} \\ \vdots \\ x_{min} \end{bmatrix}_{n(N+k_2)\times 1}, \quad H_u = \begin{bmatrix} x_{max} \\ \vdots \\ x_{max} \end{bmatrix}_{n(N+k_2)\times 1}$.

State constraints given as linear inequalities, as in Eq. (22), can be transformed in input constraints with aid of Eq.(19). For this purpose, $\hat{X}_{k_2+N}$ is initially written in terms of the control $\hat{V}$ as:

$$\hat{X}_{k_2+N} = \begin{bmatrix} \hat{X} \\ \hat{x}(k+N+1|k) \\ \vdots \\ \hat{x}(k+N+k_2|k) \end{bmatrix} = \underbrace{\begin{bmatrix} & H & & \\ \tilde{A}^N B & \tilde{A}^{N-1}B & \ldots & \tilde{A}B \\ & \vdots & & \\ \tilde{A}^{N+k_2-1}B & \tilde{A}^{N+k_2-2}B & \ldots & \tilde{A}^{k_2}B \end{bmatrix}}_{H_{N+k_2}} \hat{V} + \underbrace{\begin{bmatrix} \hat{F} \\ \tilde{A}^{N+1}x(k) \\ \vdots \\ \tilde{A}^{N+k_2}x(k) \end{bmatrix}}_{\hat{F}_{N+k_2}} \tag{23}$$

Then, Eq. (22) can be rewritten as:

$$\begin{bmatrix} \hat{X}_{N+k_2} \\ -\hat{X}_{N+k_2} \end{bmatrix} \leq \begin{bmatrix} H_u \\ -H_l \end{bmatrix} \Rightarrow \begin{bmatrix} H_{N+k_2} \\ -H_{N+k_2} \end{bmatrix} \hat{V} \leq \begin{bmatrix} H_u - \hat{F}_{N+k_2} \\ -H_l + \hat{F}_{N+k_2} \end{bmatrix} \tag{24}$$

2.3 Input Constraints

Let the control applied to the plant be given by Eq. (15). Since the input constraints are given in terms of u, they must be translated as constraints in terms of v for the optimization algorithm:

$$H_{cl} \leq \hat{U}_{k_2+N} = \begin{bmatrix} \hat{v}(k|k) - K\hat{x}(k|k) \\ \vdots \\ \hat{v}(k+N-1|k) - K\hat{x}(k+N-1|k) \\ -K\hat{x}(k+N|k) \\ \vdots \\ -K\hat{x}(k+N+k_2|k) \end{bmatrix} \leq H_{cu} \tag{25}$$

where

$$H_{cl} = \begin{bmatrix} u_{min} \\ \vdots \\ u_{min} \end{bmatrix}_{p(N+k_2)\times 1} , \quad H_{cu} = \begin{bmatrix} u_{max} \\ \vdots \\ u_{max} \end{bmatrix}_{p(N+k_2)\times 1} \tag{26}$$

in which u_{min} is the lower bound of the control and u_{max}, the upper one.

The linear inequalities expressed in Eq. (25) can be rewritten in terms of $\hat{V}$ and $x(k)$ by using Eq. (23) and rearranging:

$$H_{cl} \leq \underbrace{\left[\begin{bmatrix} I_{pN} \\ 0 \\ \vdots \\ 0 \end{bmatrix} - D^K_{N+k_2+1} \begin{bmatrix} 0 \\ H_{N+k_2} \end{bmatrix} \right]}_{S} \hat{V} - D^K_{N+k_2+1} \begin{bmatrix} x(k) \\ \hat{F}_{N+k_2} \end{bmatrix} \leq H_{cu} \tag{27}$$

in which I_{pN} is the $(pN \times pN)$ identity matrix and $D^K_{N+k_2+1}$ is a block-diagonal matrix of the form:

$$D^K_{N+k_2+1} = \begin{bmatrix} K & 0 & \dots & 0 \\ 0 & K & \dots & 0 \\ \vdots & \vdots & \ddots & \vdots \\ 0 & 0 & \dots & K \end{bmatrix}_{p(N+k_2+1)\times n(N+k_2+1)} \tag{28}$$

Finally, following the procedure used to obtain the linear inequalities over the states, the constraints on $\hat{V}$ can be expressed as:

$$\begin{bmatrix} S \\ -S \end{bmatrix} \hat{V} \leq \begin{bmatrix} H_{cu} + D^K_{N+k_2+1} \begin{bmatrix} x(k) \\ \hat{F}_{N+k_2} \end{bmatrix} \\ -H_{cl} - D^K_{N+k_2+1} \begin{bmatrix} x(k) \\ \hat{F}_{N+k_2} \end{bmatrix} \end{bmatrix} \tag{29}$$

3. METHODOLOGY

3.1 Plant Model

The simulation model used in this work was derived in (Lopes, 2007) and improved in (Maia, 2008). It is a nonlinear model for a three-degrees of freedom (3DOF) laboratory helicopter represented in the schematic design of Fig. 2 having as state variables the angles of *Travel* (T), *Elevation* (E) and *Pitch* (P), as well as their respective rates of variation $(\dot{T}, \dot{E}, \dot{P})$. The two control inputs $(u_1,\ u_2)$ correspond to the voltages applied to the power amplifiers of the front and back helicopter motors. The model obtained by (Maia, 2008) is of the form:

$$\begin{aligned} \dot{x}_1 &= x_2 \\ \dot{x}_2 &= \xi_{16} \left\{ \xi_1(u_1^2 - u_2^2) + \xi_2(u_1 - u_2) - \nu_2 x_2 \right\} \\ \dot{x}_3 &= x_4 \\ \dot{x}_4 &= x_6^2 \left\{ \xi_3 \sin 2x_3 + \xi_4 \cos 2x_3 \right\} + \xi_5 \sin x_3 + \xi_6 \cos x_3 + \left\{ \xi_7(u_1^2 + u_2^2) + \xi_8(u_1 + u_2) \right\} \cos x_1 \\ \dot{x}_5 &= x_6 \\ \dot{x}_6 &= \left\{ \xi_{13} + \xi_{14} \sin 2x_3 + \xi_{15} \cos 2x_3 \right\}^{-1} \left\{ \nu_1 - \nu_3 x_6 + \left[\xi_9(u_1^2 + u_2^2) + \xi_{10}(u_1 + u_2) \right] \sin x_1 + \right. \\ &\quad \left. x_4 x_6 \left[\xi_{11} \sin 2x_3 + \xi_{12} \cos 2x_3 \right] \right\} \end{aligned} \tag{30}$$

In Eq. (30), the states x_1, x_3 and x_5 represent the *Pitch*, *Elevation* and *Travel* angles (in radians), respectively. The values of the constants $\xi_1, \dots \xi_{16}$, ν_2 and ν_3 are adopted as the ones experimentally determined in (Maia, 2008). ν_1, however, is made equal to 0 for simplicity, resulting in an angle of 0 deg for the *Pitch* in equilibrium. Employing a first-order Taylor approximation of the nonlinear model around an equilibrium point $(\overline{x},\ \overline{u})$, a linearized model can be written as:

$$\dot{\tilde{x}} = A_c \tilde{x} + B_c \tilde{u} \tag{31}$$

where $\tilde{x} = x - \overline{x}, \quad \tilde{u} = u - \overline{u}$.

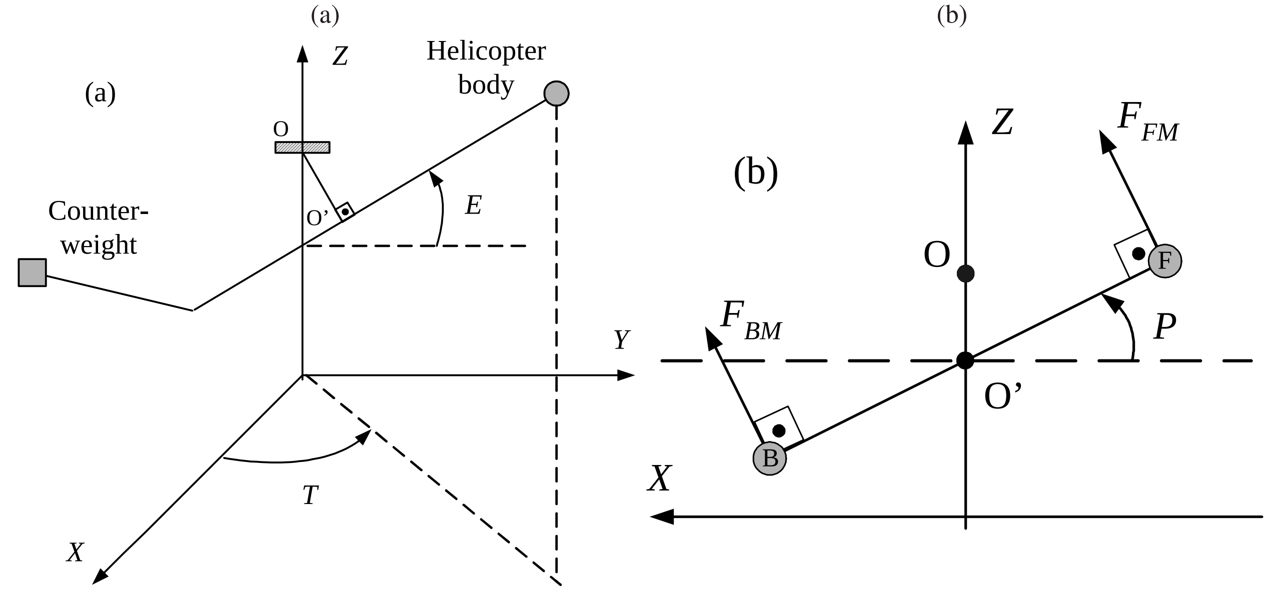

Figure 2. (a) Schematic design of the laboratory helicopter considered in this work. (b) View of the main helicopter body in the plane orthogonal to the main supporting axis. F_{FM} and F_{BM} represent the forces generated by the front and back motors, respectively.

This results in the following model matrices for an horizontal equilibrium point ($\overline{x} = 0$, $\overline{u_1} = \overline{u_2} = 2.9735\ V$):

$$A_c = \begin{bmatrix} 0 & 1.0000 & 0 & 0 & 0 & 0 \\ 0 & -0.7530 & 0 & 0 & 0 & 0 \\ 0 & 0 & 0 & 1.0000 & 0 & 0 \\ 0 & 0 & -1.0389 & 0 & 0 & 0 \\ 0 & 0 & 0 & 0 & 0 & 1.0000 \\ -1.3426 & 0 & 0 & 0 & 0 & -0.4377 \end{bmatrix}, \quad B_c = \begin{bmatrix} 0 & 0 \\ 2.966 & -2.966 \\ 0 & 0 \\ 0.4165 & 0.4165 \\ 0 & 0 \\ 0 & 0 \end{bmatrix} \tag{32}$$

In order to preserve a short notation, the tilde symbol ($\sim$) will be omitted from now on.

3.2 Internal Loop

In order to achieve zero steady-state error for the *Elevation* and *Travel* angles, integral action is inserted in these states after discretization of the linear model matrices given in Eq. (32). The resulting matrices for the augmented discrete-time model, for a sampling time $T_s = 0.040\ s$ are:

$$A = \begin{bmatrix} 1.0000 & 0.0394 & 0 & 0 & 0 & 0 & 0 & 0 \\ 0 & 0.9703 & 0 & 0 & 0 & 0 & 0 & 0 \\ 0 & 0 & 0.9992 & 0.0400 & 0 & 0 & 0 & 0 \\ 0 & 0 & -0.0415 & 0.9992 & 0 & 0 & 0 & 0 \\ -0.0011 & 0 & 0 & 0 & 1 & 0.0397 & 0 & 0 \\ -0.0532 & -0.0011 & 0 & 0 & 0 & 0.9826 & 0 & 0 \\ 0 & 0 & -1.0000 & 0 & 0 & 0 & 1 & 0 \\ 0 & 0 & 0 & 0 & -1 & 0 & 0 & 1 \end{bmatrix}, \quad B = \begin{bmatrix} 0.0023 & -0.0023 \\ 0.1169 & -0.1169 \\ 0.0003 & 0.0003 \\ 0.0167 & 0.0167 \\ 0 & 0 \\ 0 & 0 \\ 0 & 0 \\ 0 & 0 \end{bmatrix} \tag{33}$$

An internal loop with state feedback is used to stabilize the plant. The control is given as in Eq. (15) and the gain K is obtained by solving a discrete linear quadratic regulator (LQR) problem (Lewis, 1986) with weight matrices $Q_{lqr} = I_n$ and $R_{lqr} = I_p$.

3.3 Algorithm to calculate k_2

Let the linear constraints over the states be given as:

$$Sx_k \leq b, \quad k = 1, 2, \ldots \tag{34}$$

with $b \in \mathbb{R}^s$ and $b_i > 0$, $i = 1, 2, \ldots, s$.

Now define:

$$b_{min} = \min_i b_i, \quad \lambda_{max} = \max \lambda(A^T A) \tag{35}$$

The expression given in (Rawlings and Muske, 1993) to calculate the finite horizon necessary to enforce the state constraints in order to guarantee that they will be enforced at all future times is:

$$k_2 = \max \left\{ \lceil \ln \left(\frac{b_{min}}{\|S\| \, \|x_N\|} \right) / \ln (\lambda_{max}) \rceil, 0 \right\} \tag{36}$$

where $\lceil z \rceil$ denotes the smallest integer that is still larger than z. However, the value of $x_N = \hat{x}(k+N|k)$ is not known before the optimal control is calculated. In the present paper, the following algorithm is proposed to circumvent this problem:

ALGORITHM CALCULATE_k_2
1 Let $k_2 = \infty, \ k_3 = 0$
2 **while** $k_2 \neq k_3$ **do**
3 $k_2 = k_3$;
4 Solve Quadratic Programming problem with state constraints until $N + k_2$;
5 Use the linearized model to obtain x_N employing the control obtained in step 4;
6 Let $k_3 = \max \left\{ \lceil \ln \left(\frac{b_{min}}{\|S\| \|x_N\|} \right) / \ln (\lambda_{max}) \rceil, 0 \right\}$;

In the simulations described in the next section, this algorithm typically converged in less than three iterations.

3.4 Simulation Scenarios

For comparison of performance and robustness of both MPC formulations (with finite and infinite-horizons), a control horizon of $N = 50$ steps (i.e. $2\ s$, with the sampling time $T_s = 0.040\ s$) was adopted, after which the MPC control v is set to zero. For the finite horizon approach, the prediction horizon adopted is also of 50 steps. The helicopter is initially at rest at a *Travel* position of -10 deg and the objective is to bring the helicopter to the equilibrium point $P = T = E = 0$ deg. The weights of the inputs and states in the cost were made equal and the same in both cases ($Q = I_n$ and $R = I_p$).

The constraints were imposed over the inputs (voltage applied to the front and back motors), which are the same for both motors and must remain in the interval $[0,\ 5\ V]$. Moreover, it is desirable to limit the *Pitch* angle, as would occur in a real flight situation. The constraints over the *Pitch* angle are so that it must remain in the interval $[-10\ \text{deg},\ 10\ \text{deg}]$. However, in order to guarantee that the *Pitch* angle remains within this interval, tighter constraints are imposed ($P \in [-9\ \text{deg},\ 9\ \text{deg}]$) to allow for small violations in case of infeasibility of the optimization problem. This procedure is in accordance with the separation between operational and physical constraints (Afonso and Galvão, 2007), (Alvarez and Prada, 1997). The first represent physical bounds related to the capabilities of the plant and should never be violated, and the latter are defined by the operator to obtain a desired behavior. Tighter constraints may be used to avoid the violation of looser ones, because the solution tends to be less aggressive in terms of proximity to the bounds. In order to solve the optimization problem, the `quadprog` function of the Optimization Toolbox of Matlab was employed. In case of infeasibility, the `quadprog` function returns a solution that minimizes the maximum distance to the violated constraint boundaries (Afonso and Galvão, 2007), which may lead to a non-admissible control value. Therefore, a saturation was placed on the control, so that it remains within the allowed interval.

Robustness was evaluated through a simulated failure in the back motor. Such a failure consists of a change in the gain of the voltage applied to the power amplifier of this motor, which, for illustration purposes corresponded to a drop of 0 to 30% in constant steps of 10%. The results of both controllers were evaluated and the *Travel* angle was chosen for performance analysis. The enforcement of constraints was also considered. All simulations were carried out for a period of $15\ s$. A Fourth-order Runge-Kutta solver with fixed step size $T_s/10$ was employed for simulation of the nonlinear model.

4. RESULTS

Figure 3 presents the *Pitch* and *Travel* angles obtained in the closed-loop simulation with nominal gain. It can be noted in Fig. 3a that both controllers violate the lower bound for the *Pitch* angle (-9 deg), possibly because of model-plant mismatch, since the model used for prediction is linear and the one used in the simulation is nonlinear. Nevertheless, the actual desired constraint (-10 deg) is enforced by the infinite-horizon controller as shown in the inset of Fig. 3a. Figure 3b shows the behavior of the *Travel* angle. As can be seen, both controllers achieve the desired equilibrium condition without steady-state error. However, the infinite-horizon controller results in a response with smaller overshoot and settling time.

(a) (b)

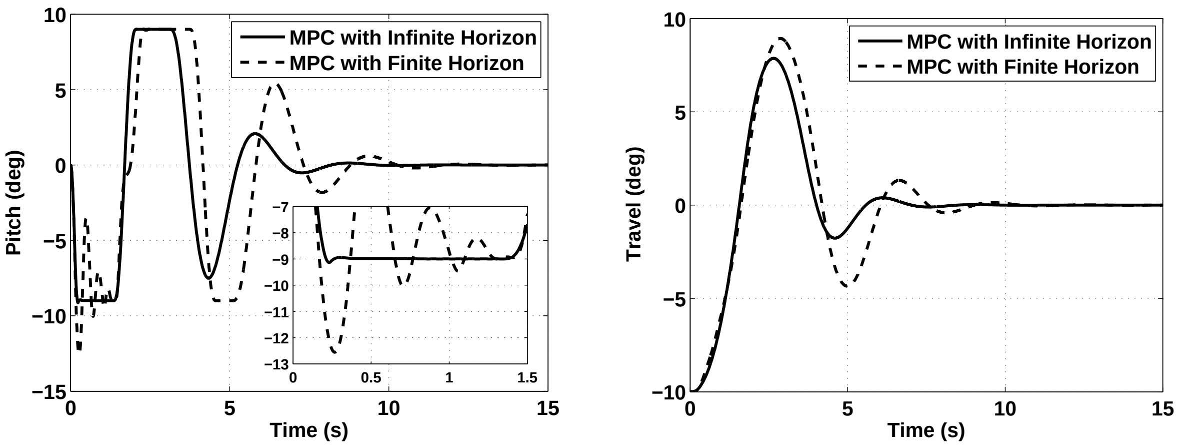

Figure 3. (a) *Pitch* and (b) *Travel* angle responses obtained in the simulation with nominal gain for both infinite (continuous line) and finite (dashed line) horizon approaches.

Figure 4 depicts the control voltages applied to the motors after saturation to the interval $0 - 5V$. It is worth observing that the infinite-horizon controller generates a smoother control signal, with less pronounced variations as compared to the finite-horizon controller. Such a feature would be of value for the actual implementation of the predictive control law, as a smoother control signal will place a smaller demand on the power amplifiers that drive the helicopter motors.

(a) (b)

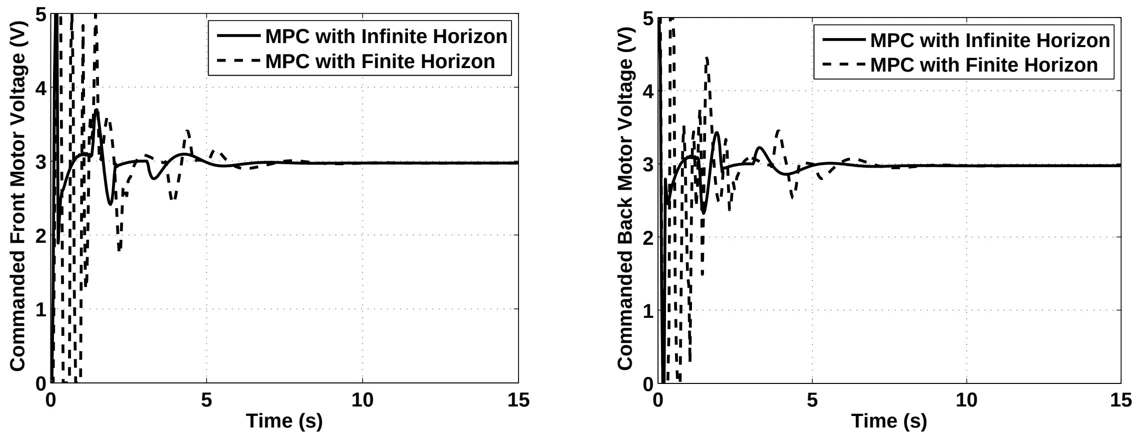

Figure 4. (a) Front and (b) back motor voltages obtained in the simulation with nominal gain for both infinite (continuous line) and finite (dashed line) horizon approaches.

For comparison purposes, Table 1 presents some indices broadly used in control for comparison of different approaches. These are: the overshoot (M_p); rise-time ($t_r|_0^{100\%}$); and Sum of Squared Errors for the Travel (SSE_T) angle, and the voltages applied to the front (SSE_{u_1}) and back (SSE_{u_2}) motors, all with respect the equilibrium values of these variables. It is worth noticing that the infinite horizon MPC approach outperforms the finite one regarding all indices.

Table 1. Comparison indices for performance of both controllers with nominal actuator gain

MPC Approach	M_p	$t_r\|_0^{100\%}(s)$	$SSE_T(\deg^2)$	$SSE_{u_1}(V^2)$	$SSE_{u_2}(V^2)$
Finite Horizon	89.3%	1.61	5.16×10^4	1867	1469
Infinite Horizon	78.6%	1.56	4.12×10^4	367	350

Both MPC approaches were subjected to tests where the back motor voltage gain was reduced. Figure 5 shows a comparison between the cases with nominal voltage gain and voltage gain reduced by 30% with respect to the nominal value. As can be seen, the gain mismatch has little effect on the overshoot and settling time with the infinite-horizon method. In contrast, the finite-horizon method has a substantial degradation in performance.

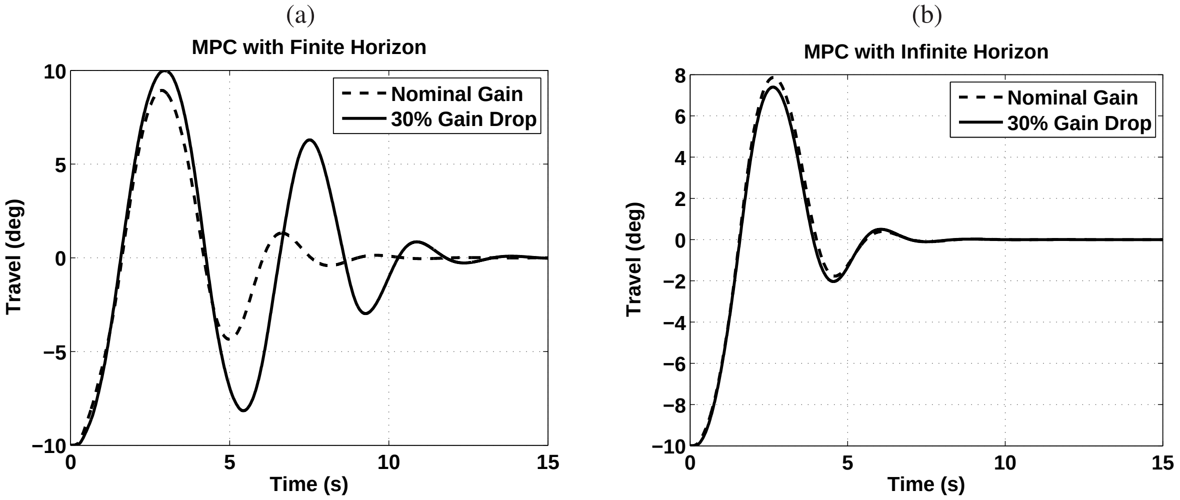

Figure 5. (a) *Travel* angle responses for finite and (b) infinite-horizon approaches obtained in the simulation with nominal gain (continuous line) and a 30% drop in the back motor voltage gain (dashed line).

In order to have a comparison criterion for robustness of the controller, the root mean square (RMS) value of the difference between the *Travel* angle response with nominal gain and with reduced gain was calculated for different values of voltage gain drop in the back motor. The results presented in Table 2 demonstrate a superior performance of the infinite-horizon approach. The RMS deviation from the nominal response for this approach is at most 51.0% of the correspoding value obtained with the finite-horizon MPC controller. As expected, in both cases the RMS value becomes larger as the gain is made smaller.

Table 2. RMS values of the deviation from the nominal *Travel* angle response

Back motor voltage gain drop	$RMS_{infinite}$	RMS_{finite}	$RMS_{infinite}/RMS_{finite}$
10%	1.57	3.08	0.510
20%	3.05	9.95	0.306
30%	4.72	45.72	0.103

Figure 6 presents the computational time demanded by the MPC calculations at each sampling period, normalized by the minimum value obtained with the finite-horizon method. The times presented in this figure correspond to the average of 10 runs for the nominal case (without gain mismatch). As can be seen, the infinite-horizon approach is more demanding in terms of computational effort, as compared to the finite-horizon formulation. However, such an additional effort may be justifiable to obtain greater robustness with respect to actuator faults, as shown in the case study.

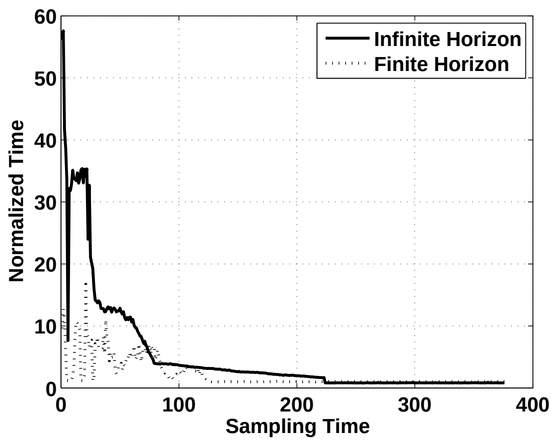

Figure 6. Computational time demanded at each sampling time for the infinite (continuous line) and finite (dotted line) horizon approaches.

5. CONCLUSION

The results obtained in this work show that the infinite-horizon MPC formulation provided smaller overshoot and settling time as compared to the finite-horizon approach. In addition, the infinite-horizon MPC controller was found to be superior to the finite-horizon one when it comes to robust performance. Through simulation of a 3DOF-helicopter using a nonlinear model and actuator gain mismatch, it was observed that such a mismatch has greater effects on the performance of the finite horizon controller. Although the infinite-horizon approach is more demanding in terms of computational workload, its use may be justifiable to obtain greater robustness with respect to actuator faults. Additional investigation would be required to establish conditions for convergence of the algorithm presented in subsection 3.3. However, the case study suggests that the algorithm is a valid heuristic, in that convergence was typically achieved in less than three iterations.

These results motivate the use of infinite-horizon MPC as an advantageous alternative to the finite-horizon formulation. Further studies concerning the handling of constraint violations might be of interest, in order to extend previous investigations involving the finite-horizon approach (Afonso and Galvão, 2007).

6. ACKNOWLEDGEMENTS

The authors acknowledge the support of FAPESP (grants 2008/10229-7 and 2006/58850-6), CNPq (research fellowship) and CAPES (Pró-Engenharias).

7. REFERENCES

Afonso, R. J. M. and Galvao, R. K. H., 2007, "Predictive control of a magnetic levitation system with infeasibility handling by relaxation of output constraints", ABCM Symposium Series in Mechatronics, Vol. 3, pp. 11 – 18.

Alvarez, T. and Prada, C., 1997, "Handling infeasibilities in predictive control", Computers in Chemical Engineering, Vol. 21, pp. S577–S582.

Camacho, E.F., Bordons, C., 1999, Model Predictive Control. Springer-Verlag. London.

Chisci, L., Rossiter, J. A. and Zappa, G., 2001,"Systems with persistent disturbances: Predictive control with restricted constraints", Automatica, Vol.37, pp. 1019–1028.

Cutler, C. R. and Ramaker, B. L., 1980, "Dynamic matrix control - a computer control algorithm", Proceedings of the Joint American Control Conference, San Francisco, 1980.

Keerthi, S. S. and Gilbert, E. G., 1988 "Optimal infinite-horizon feedback laws for a general class of constrained discrete-time systems: stability and moving-horizon approximations", Journal of Optimization Theory and Applications, Vol. 57, No. 2, pp. 265–293.

Lewis, F. L., 1986, " Optimal Control", A Wiley Interscience Publication. New York.

Lopes, R. V., 2007, "Modelagem e Controle Preditivo de um Helicóptero com Três Graus de Liberdade", Master's thesis. ITA. São José dos Campos.

Maciejowski, J.M., 2002, "Predictive Control with Constraints", Prentice Hall. Harlow, England.

Maia, M. H., 2008, "Controle Preditivo Robusto de um Helicóptero com Três Graus de Liberdade Sujeito a Perturbações Externas", Master's thesis. ITA. São José dos Campos.

Mayne, D. Q., Rawlings, J. B., Rao, C. V. *et al.*, 2000, "Constrained model predictive control: Stability and optimality", Automatica, Vol. 36, No. 6, pp. 789 – 814.

Muske, K. R. and Rawlings, J. B., 1993, "Model predictive control with linear models", AIChE Journal, Vol. 39, No. 2, pp. 262 – 287.

Qin, S. J. and Badgwell, T. A., 2003, "A survey of industrial model predictive control technology", Control Engineering Practice, Vol. 11, No. 7, pp. 733–764.

Rawlings, J.B. and Muske, K.R., 1993, "The stability of constrained receding horizon control", IEEE Transactions on Automatic Control, Vol. 38, No. 10, pp. 1512–1516.

Rossiter, J. A., 2003, "Model-based predictive control", CRC Press, Boca Raton, 2003.

Scokaert, P.O.M. and Rawlings, J.B., 1999, "Feasibility issues in linear model predictive control", AIChE Journal, Vol. 45, No. 8, pp. 1649–1659.

8. RESPONSABILITY NOTICE